12th AIAA/CEAS Aeroacoustics Conference (27th AIAA Aeroacoustics Conference)
8-10 May 2006, Cambridge, Massachusetts

AIAA 2006-2705

Effect of microjets on a high-subsonic jet. Parametric study of far-field noise reduction.

Thomas Castelain, Michel Sunyach, Daniel Juvé

Laboratoire de Mécanique des Fluides et d'Acoustique,CNRS UMR 5509, Ecole Centrale de Lyon

36 Avenue Guy de Collongue 69134 ECULLY Cedex, France

and Jean-Christophe Béra

INSERM U556, Université Claude Bernard Lyon I, Lyon, France

A system of 36 impinging microjets was implemented on a Mach=0.9 round jet, and the noise reduction was studied as a function of the microinjection mass flux, the number of microjets blowing, the layout of the blowing microjets, and the microjet diameter. Depending on the microinjection flow parameters, the global jet-noise reduction varied from 0 to 1.8 dB, showing some non-monotonic behaviors due to the change between subsonic and supersonic regimes of the microjets. The study of the layout of the microjets shows that the noise reduction decreases when the microjets are too close to each other and that some configurations of microjet pairs could be favourable, which can be linked to the flow structures induced by the microjets. Spectral analyses pointed out different mechanisms involved in the control, with a high-frequency regeneration for high injections, a local behavior of the control at the mid-frequencies and a global behavior at the low-frequencies.

Introduction

Noise generation from high-speed turbulent jets remains a significant research topic, due to its crucial implication in the aeronautical industry. The growth of airplane trafic and the increase of the number of airports, associated with always more restrictive norms, are some present arguments to continue the effort on this subject. Despite experiments and numerical simulations on jets carried out over the last few decades, the fundamental mechanisms underlying the jet noise have still to be determined. For supersonic jets, the feed-back loop mechanisms in the noise generation have satisfactorily been described (Tam[1]) and a good agreement between theory and experiments has been obtained for pure tone noise. The comprehension of the jet mixing noise, occuring both in supersonic and high-subsonic jets, still remains a challenge.

Recently, a micro-injection system impacting with air the main jet has been suggested (Arakeri *et al.*,[2] Castelain *et al.*[3]). The benefits of such a system are a reduction of the level of turbulence in the mixing layer and a reduction of the noise spectra level for all angles of directivity. The reduction level relies on the jet Mach number M_j, and on parameters concerning the micro-injection. The present study focuses on the effect of injected mass flux, the number of microjets, the microjets layout, and the microjet diameter.

Experimental set-up

The experiments were carried out in the supersonic anechoic facility of the Centre Acoustique, LMFA - École Centrale de Lyon. The jet has a diameter D of 50 mm and is powered by a centrifugal compressor of 450 kW with a maximum mass-flux of 1 kg.s^{-1}. After compression, the air was heated by a set of resistances of total power 80 kW, to set the temperature of the jet after the expansion to room temperature. The results presented here concern a jet at a Mach number based on the external speed of sound c_0 of $M_j = 0.9$.

The control system is made of up to 36 microjets directed toward the jet centerline and impacting the jet with a 0° yaw angle (Figure 1(a)). Three sets of microjets are used; the first set is composed of 18 brass tubes with removable nozzles of different diameters (Figure 1(b)). This set of microjets was uniquely used to study the effect of the microjet diameter. The second set is composed of 36 straight brass tubes of 1 mm exit diameter and the third set of 36 brass tubes with a final bend of 22°. This third geometry was used to study the effect of the impinging angle.
The microjets are fed by a piston compressor, connected to a relief valve and two pressure distributors feeding 18 microjets each. To impose a given mass flux through the microjets, the static pressure is monitored in each distributor with a 0-60*PSI* Honeywell XCA460an pressure sensor.
The noise spectra are obtained with two B&K 4192 1/2" microphones and a B&K Nexus Power Supply, connected to a PXI-1006 spectrum analyser with PXI-4472 Acquisition cards set with a sampling rate of $f_e = 81920$ Hz. The spectra results from the averaging of 400 samplings of 16384 points each. The overall Sound Pressure Levels (SPL) are computed by integrating the spectra from f_1=200 Hz to f_2=35 kHz, with a reference pressure $p_{ref} = 2.10^{-5}$ Pa. The microphones are located at 40 D from the jet exit centre, and θ is the angle between the downstream jet axis and the microphone.

a) Typical layout with 1mm straight microjets

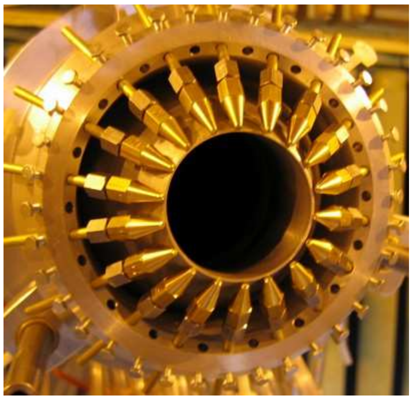

b) Configuration used for the study of microjet diameter d.
(d=0.7mm, 1mm and 1.3mm)

Fig. 1 Experimental set-up

Measurement repeatability

According to previous studies (Gutmark *et al.*,[5] Castelain *et al.*[4]), the typical high-subsonic jet noise reduction with microjets is 1 to 2.5 dB. Moreover, the difference in noise reduction for two given microjet configurations is typically of 0.2 dB. The parametric approach proposed here is then relevant only whether the measurement repeatability is less than the typical value of 0.2 dB, which implies extreme cares of the measurement conditions. The jet Mach number uncertainty is below 5.10^{-3}, and the jet temperature uncertainty is below 2°C.
The noise spectra for the reference jet, *i.e.* without control, were acquired regularly during each test. The typical R.M.S value of the sound pressure level variation during one test is 0.02 dB for $\theta = 90°$ and 0.04 dB for $\theta = 30°$, which perfectly meets the specifications. In the other hand, the comparisons between tests carried out on different days give a difference between the associated SPL of about 0.2 dB, which could result from slightly different jet Mach numbers in the uncertainty range or variations of atmospheric conditions. As the comparison between the microjet systems may imply several tests, the procedure for comparison is then the following : the noise reduction brought by a configuration

of microjets is calculated relatively to the SPL of the reference jet measured during the same test, and the comparison between the different configurations is based on the assumption that the noise reduction is unaffected by the slight changes in reference jet SPL.

Microjets configurations

The microjets were set in the circumference of the main jet at the nozzle exit, previously demonstrated to be the optimal longitudinal distance of injection (Castelain *et al.*[4]). The microjets were systematically maintained at the nozzle exit for all the impinging angles tested, by means of a translatory motion of the entire microjet system. The microjets were regularly set every 10° degrees, so that the maximum number of blowing microjets was 36.

Effect of the injected mass flux

The type of the 18 microjets used in this section is illustrated in Figure 1(a) and corresponds to the second type mentionned above. The impacting angle is 45°. The mass flux per microjet were varied by changing the upstream pressure by means of the relief valve. The monitoring of the static pressure in the pressure distributor ensures a mean variation of the injected mass flux during the acquisition below 1%. The injected mass flux is considered in the following in terms of mass flux ratio r_m between the injected mass flux per microjet and the main jet mass flux.

Figure 2(a), respectively 2(b), gives the SPL reduction brought by the 18 microjets with r_m for $\theta = 30°$, respectively $\theta = 90°$. For the two angles, the global trend is an increase of the SPL reduction with the mass flux ratio; we also notice the presence of a local maximum located at $r_m = 3.3\ 10^{-4}$, followed by a local minimum at about $r_m = 5\ 10^{-4}$ after which the SPL reduction is a monotonic increasing function of the mass flux, in the range of mass flux under the scope of this study.

We first compare the configurations apart from the local maximum, giving the same SPL reduction. The □ symbols on Figure 2(a) highlight two different r_m giving approximately equal noise reductions for $\theta = 30°$. The corresponding noise reductions for $\theta = 90°$ are indicated in the same way on Figure 2(b). The corresponding mass flux ratio are $r_m^1 = 2\ 10^{-4}$ and $r_m^2 = 5.5\ 10^{-4}$.

Figures 2(c) and 2(d) gives the Power Spectrum Densities corresponding to these two values of the mass flux ratio for $\theta = 30°$ and $\theta = 90°$. These PSD can be compared with the PSD of the reference jet, plotted in red. For $\theta = 30°$, the reductions in the low frequency range of the spectra are identical for the two values of r_m. As this frequency range contains most of the acoustic energy, this justifies the equality of the SPL between these two cases. In the range 5 kHz - 15 kHz, we observe that the highest spectral reduction is obtained for $r_m = r_m^2$. Above 15 kHz we notice a higher noise regeneration for $r_m = r_m^2$. For $\theta = 90°$, the above conclusions are applying too; the only difference is the narrower dynamics of the jet noise for this value of θ than for $\theta = 30°$. As a consequence, the spectral reduction in the low-frequency range is not determining the global noise reduction as this is the case in the $\theta = 30°$ case. The spectral components in the range 5 kHz - 15 kHz are contributing in that case to the SPL. Thus, the best configuration is the one corresponding to $r_m = r_m^2$.

The singularity of the local maximum excepted, we observe an increase in the noise reduction with the mass flux ratio. Three values of r_m, increasingly named r_m^α, r_m^β, r_m^γ, illustrate that trend on Figures 2(a) and 2(b) with circles marks. The corresponding spectra, given in Figures 2(e) and 2(f), indicates that the highest spectral reduction in the low frequency range is achieved by the configuration with the highest mass flux ratio r_m^γ, to the detriment of a higher noise regeneration in the high frequency domain. Regarding the dynamics of the jet noise and the scale of the laboratory jet studied here, this high frequency noise is clearly insignificant regarding the SPL; for a larger jet diameter and a EPNdB-weighting - in other words for flight certification - what we call here high frequency noise regeneration might then become significant.

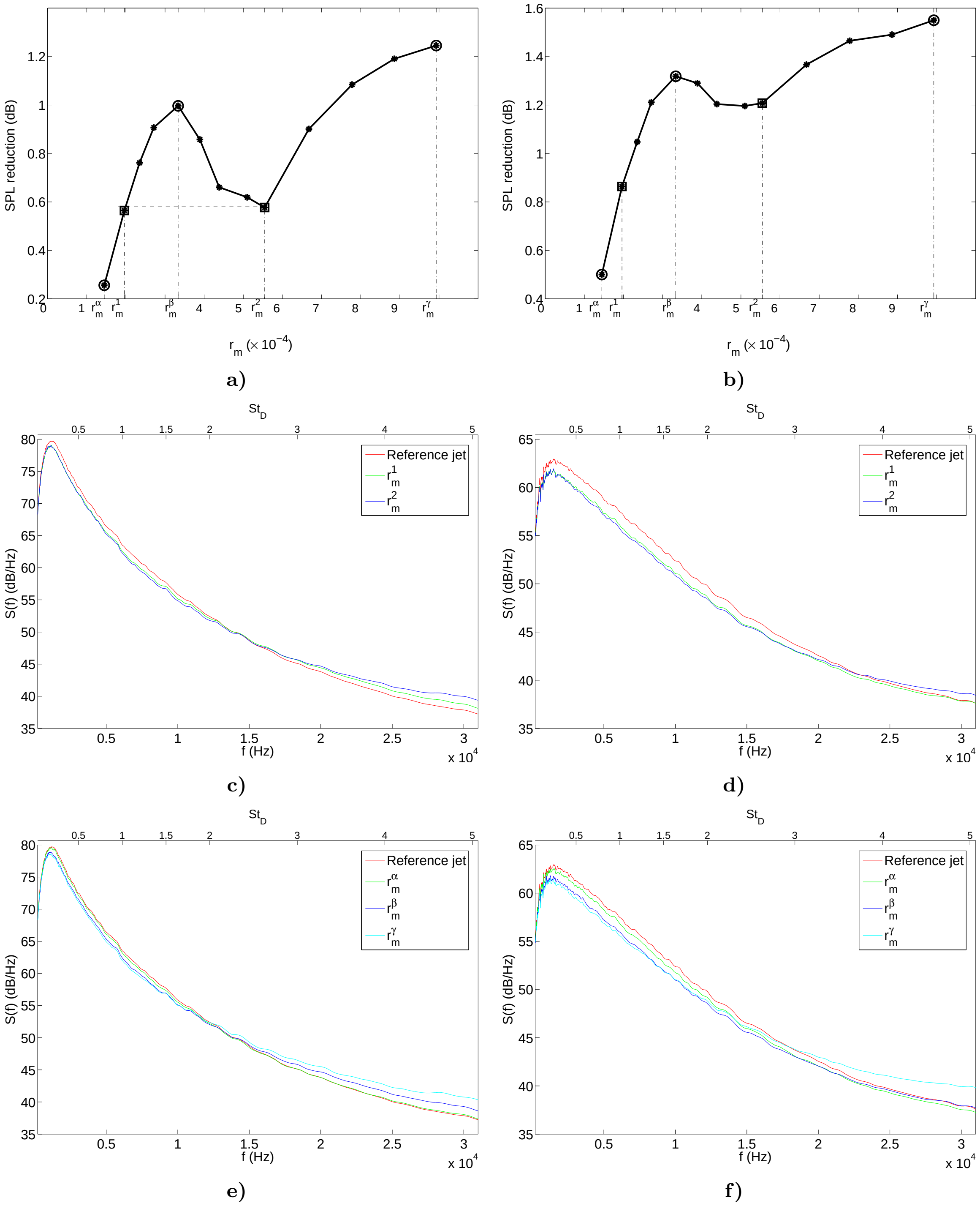

Fig. 2 Evolution of the SPL reduction with the mass flux ratio per microjet, (a) for $\theta = 30°$ and (b) for $\theta = 90°$.
The Power Spectrum Densities corresponding to the □ marks are given as a function of frequency f and Strouhal number St_D based on jet diameter D : Figure (c) for $\theta = 30°$ and (d) for $\theta = 90°$; the ◯ marks are illustrated in Figure (e) for $\theta = 30°$ and (f) for $\theta = 90°$.
Jet Mach number $M_j = 0.9$; Number of microjets : 18; Impacting angle : 45°.

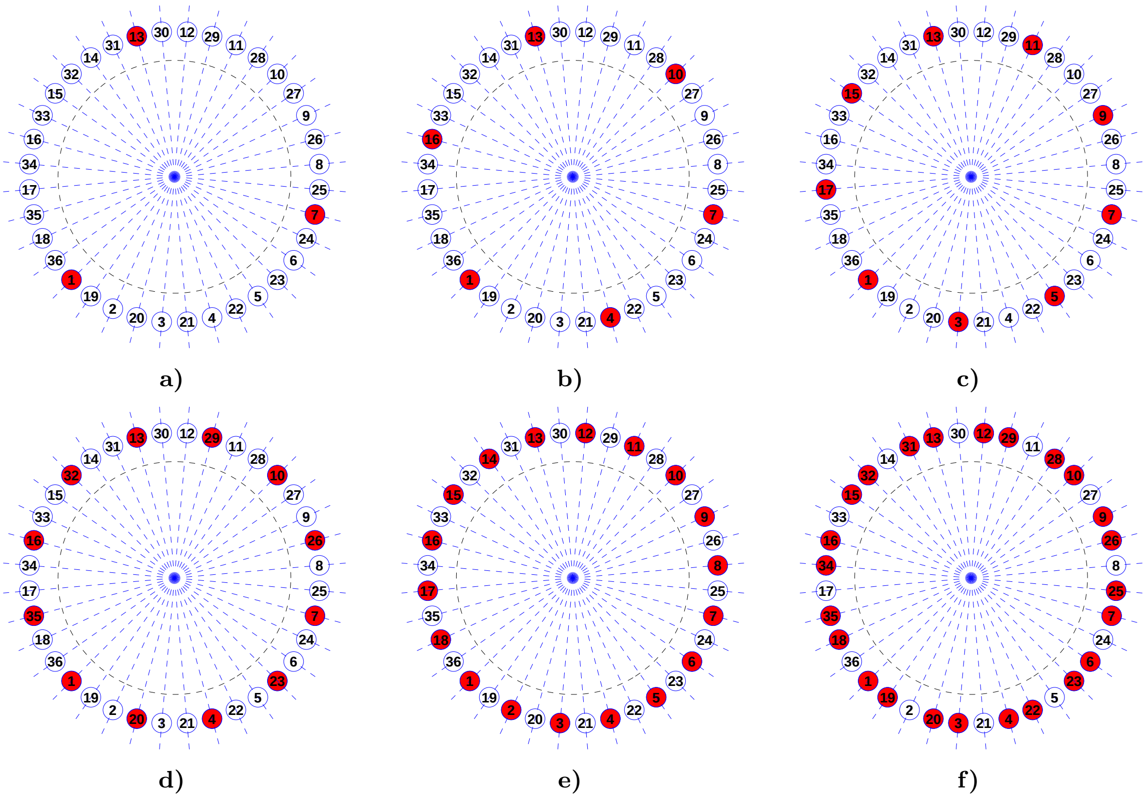

Fig. 3 Configurations tested by varying the number of microjets. Each microjet is represented by a blue circle, colored with red if the microjet is blowing. The number attributed to each microjet depends on the pressure distributor connected ; the microjets with the numbers 1 **to** 18 **are connected to the first pressure distributor, and the microjets with the numbers** 19 **to** 36 **to the second one.**

Effect of the number of microjets

Different numbers of microjets have been tested, from 36 to 3. Figure 3 illustrates the tested configurations which are maintaining an axisymmetric distribution of the microjets. The configuration where all the microjets are blowing, not represented on Figure 3, was also tested.
Figures 4(a) and 4(b) relate the evolution of the SPL reduction with the number of blowing microjets n, for a given value of the mass flux ratio $r_m = 2.7\ 10^{-4}$. We observe the presence of a maximum reduction for $n = 18$, while the configuration with $n = 36$ gives a SPL reduction at $\theta = 30°$ equivalent to the one obtained by use of $n = 6$. The spectra corresponding to these three configurations are given in Figures 4(c) and 4(d). If the reduction in low frequencies is directly linked to the SPL reduction, the contribution of the different configurations to the noise reduction in the mid-frequencies and the high frequencies provides additional informations. Indeed, we can observe that the high-frequency noise regeneration, clearly visible on Figure 4(c), appears for $f = 15kHz$ in the case of $n = 6$ and $n = 18$ microjets configurations, whereas this phenomenon is shifted to $f = 20kHz$ in the case of $n = 36$ microjets. The differences between those three configurations may then be correlated with different scales of the structures resulting from the interaction between the jet mixing layer and the microjets ; a close microjets spacing may create an interaction between two adjacent microjets, potentially causing the modification of the scales of the generated structures.

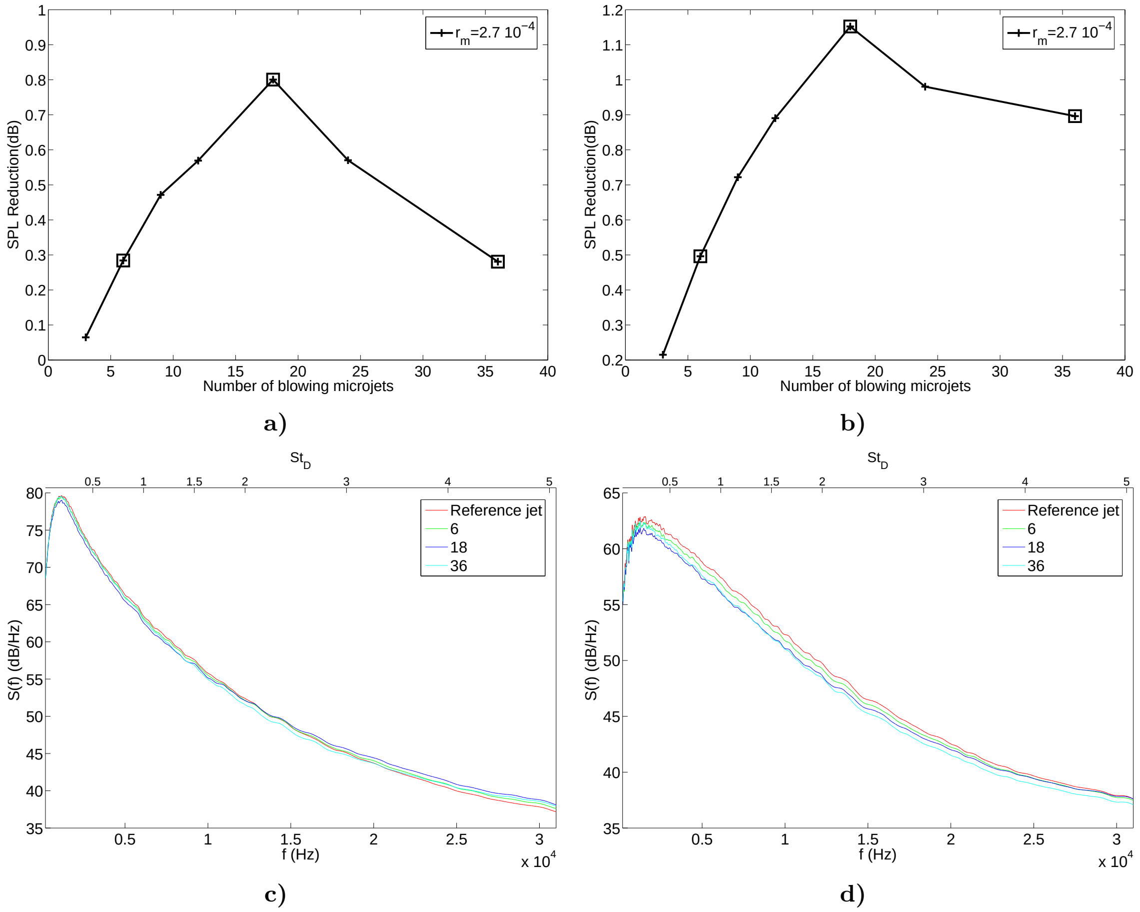

Fig. 4 Evolution of the SPL reduction with the number of microjets, for a mass flux ratio per microjet $r_m = 2.7\ 10^{-4}$; (a) $\theta = 30°$, (b) $\theta = 90°$. The Power Spectrum Densities corresponding to the reference jet and the □ marks, *i.e.* $n = 6$, $n = 18$ and $n = 36$, are given in (c) for $\theta = 30°$ and (d) $\theta = 90°$, as function of frequency f and Strouhal number St_D based on jet diameter D. Jet Mach number $M_j = 0.9$; Number of microjets : 3 to 36 ; Impacting angle : 45°.

Figure 5 gives the evolution of the SPL reduction with the mass flux ratio per microjet r_m, for $n = 12$, $n = 18$ and $n = 36$. A similar trend is observed for $n = 12$ and $n = 18$, with the presence of a local maximum as described in the previous section. That trend has been observed for the $n = 3$, $n = 6$, $n = 9$ configurations too. The $n = 18$ configuration is less efficient than the $n = 12$ one in terms of noise reduction for r_m greater than, which possibly illustrate the microjets interaction mentionned above. In the other hand, the $n = 24$ microjets configuration is the only known configuration to provide a monotonic SPL reduction with r_m ; moreover, the SPL reduction obtained with that configuration for sufficiently high r_m is the maximum reached in this study. As a consequence, we may infer that the pairing of microjets possibly act on the jet mixing layer with mechanisms different of those implied with single microjets.

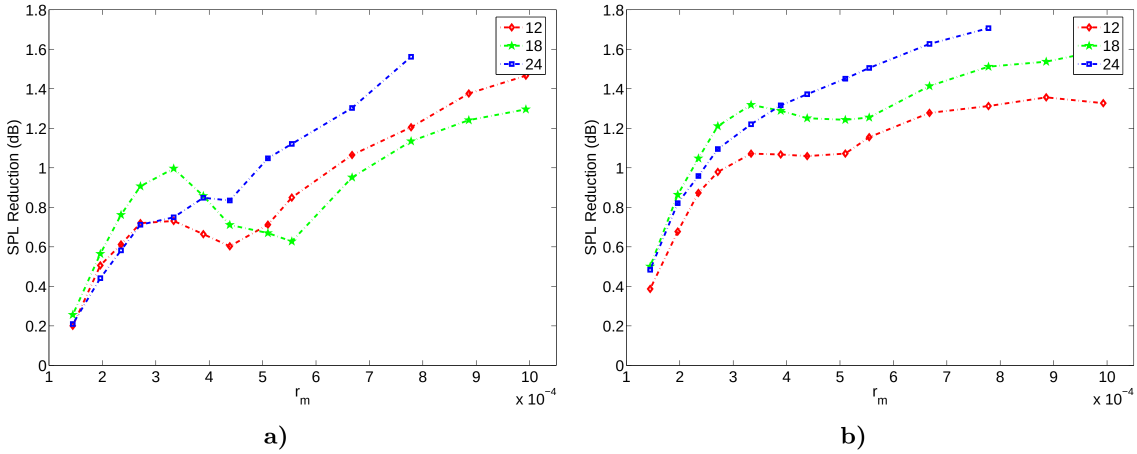

Fig. 5 Evolution of the SPL reduction with the mass flux ratio per microjet, for $n = 12$, $n = 18$ and $n = 24$ blowing microjets.
Jet Mach number $M_j = 0.9$; Number of microjets : 3 to 36 ; Impacting angle : 45°.

Effect of the microjets layout

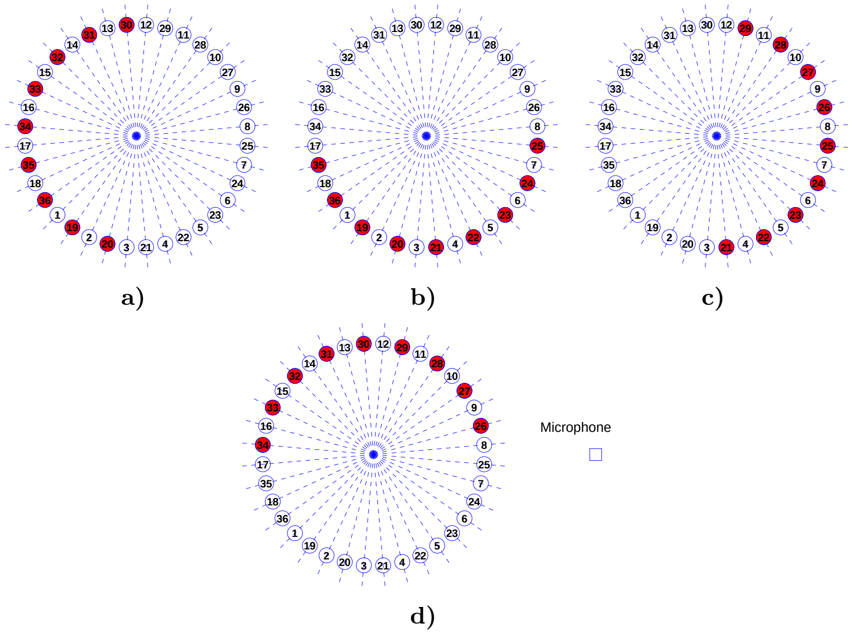

Fig. 6 Different layouts tested for 9 microjets.

In this section, the parameter of interest is the geometrical layout of the microjets regarding the microphones. Figure 6 illustrates the position of 9 microjets towards the microphone, located as illustrated on Figure 6(d). Thus, in the following, the configuration represented in Figure 6(c) is called the close 9 microjets configuration, and the one represented in Figure 6(a) is called the opposite 9 microjets configuration.

The tests were carried out with the configuration of Figure 3(c) with 9 microjets axisymmetrically distributed and with the 4 configurations listed on Figure 6 implying 9 adjacent microjets. To complete the study, the configuration including 18 microjets of Figure 3(e) was also considered. The SPL reduction brought by the different configurations are given in Figure 7(a) for $\theta = 30^\circ$ and in Figure 7(b) for $\theta = 90^\circ$. Each curve represents the SPL for the natural jet (*i.e.* the first point of each curve), the 4 configurations with 9 adjacents microjets (*i.e.* the four following points of each curve) and the configurations with 9 microjets distributed around the main jet (*i.e.* the fifth point of each curve) and 18 microjets (*i.e.* the sixth point of each curve). Three different mass flux per microjet are represented, providing three curves for each angle of directivity.

The configurations with 9 adjacent microjets are providing approximately the same SPL reduction for a given mass flux per microjet. The only major difference is obtained when comparing the opposite 9 microjets configuration (Figure 6(a)) to the close 9 microjets configuration (Figure 6(c)) in the case of a high mass flux per microjet. The difference in SPL reduction between the former and the latter is then about 0.3 dB.

Moreover, for all the tested values of mass flux, the configuration with 9 distributed microjets (Figure 3(c)) is more efficient than the configurations with 9 adjacent microjets. In the case of a high mass flux per microjet, the SPL reduction is almost doubled by distributing the 9 microjets in comparison with a 9 adjacent microjets configuration at $\theta = 30^\circ$ as well as at $\theta = 90^\circ$. An increase in the SPL reduction is obtained by using a 18 microjets configuration (Figure 3(e)).

The associated spectra for a high mass flux per microjet are given in Figure 7(c) and Figure 7(d). For clarity reasons, the spectra considered are the product of the frequency with the Power Spectrum Density (PSD) of the microphone signal, $fS(f)$. Details on the advantages of that formalism are given in Castelain *et al.*[4]. Figures 7(c) and 7(d) compares the differences $\Delta[fS(f)]$ between the reference jet noise spectrum and the spectra corresponding to different microjets layouts, *i.e.* $\Delta[fS(f)] = [fS(f)]_{reference\ jet} - [fS(f)]_{controlled\ case}$. The represented spectra concern the 9 adjacent microjets configurations, the 9 distributed microjets configuration and the 18 microjets configuration.

Figure 7(d) illustrates the results obtained in SPL reduction for $\theta = 90^\circ$. For all the microjets configurations, the noise reduction is obtained for the entire frequency range from 200 Hz to 35 kHz. The similarity between the noise reduction obtained with the 4 adjacent microjets configurations are illustrated by the proximity of the different related $\Delta[fS(f)]$.

For $\theta = 30^\circ$, Figure 7(c) illustrates the noise reduction obtained for the frequency range from 200 Hz to 10 kHz. Above that frequency, noise regeneration exists but is not visible because of the linear scale for $\Delta[fS(f)]$. Comparing the 4 adjacent microjets configurations, we obtain that the close 9 microjets configuration brings a higher noise reduction than the opposite configuration for the entire frequency range. By taking into account the axisymmetrically distributed microjets configurations, we observe a similar trend for frequency above 3kHz, between the 18 distributed microjets and the close configuration in the one hand, and between the 9 distributed microjets and the other adjacent microjets configurations in the other hand. In this case of high mass flux per microjet and for $\theta = 30^\circ$, a directionnal effect of noise reduction is then obtained, resulting first from a modification of the noise reduction in the low frequency range and secondly in the high frequency range with no effect on the SPL. The similarity in high frequency between the 18 distributed microjets and the close 9 microjets configuration could characterize a local effect of microjets, knowing that in these two configurations the number of microjets on microphone side are equal. The major difference in SPL reduction for $\theta = 30^\circ$ between the adjacent microjets configurations and the distributed one, resulting from differences in the low-frequency range, may illustrate a global effect of the control.

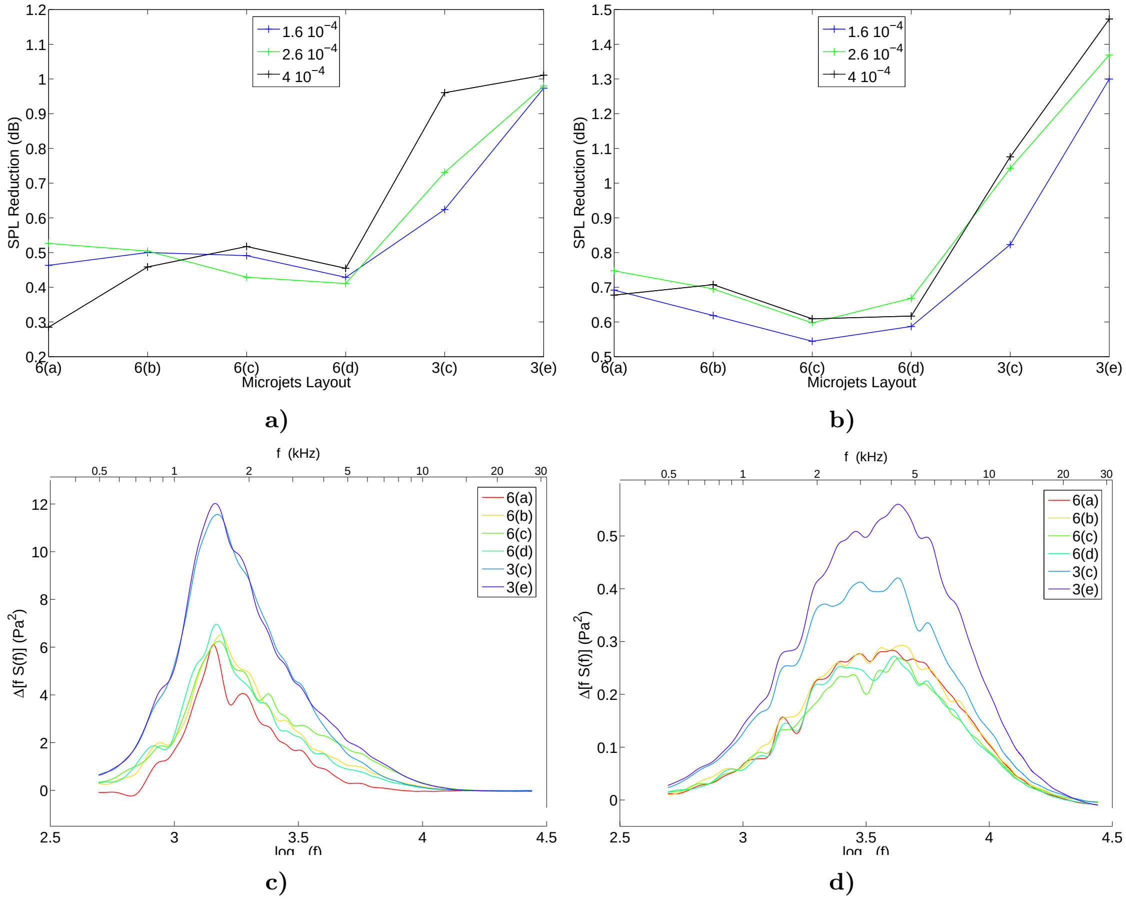

Fig. 7 Evolution of noise reduction for different microjet layouts with 9 microjets, and comparison with the case of 18 microjets. The layout are mentionned by their corresponding illustrating Figure number. The SPL reductions are given in (a) for $\theta = 30°$ and (b) for $\theta = 90°$; Associated $\Delta[fS(f)]$, *i.e.* the difference between the frequency-weighted spectrum of the reference jet and the spectrum of the control cases, are given for $\theta = 30°$ (c) and $\theta = 90°$ (d), for $r_m = 4\ 10^{-4}$.

Effect of the microjet diameter

The microjet system used for this study is illustrated on Figure 1(b). This system involves 18 microjets made of brass tubes with threaded endings to receive screwed nozzles of different diameters. This set-up ensures that the geometrical settings remain unchanged between the different tests. The diameters under the scope of this study are respectively 0.7mm, 1mm and 1.3mm.

Figure 8(a), respectively 8(b), represents the evolution of the noise reduction with the mass flux per microjet ratio for $\theta = 30°$, respectively for $\theta = 90°$. Each curve represents the results obtained with a given microjet diameter d.

We observe the same trend for the results obtained with the three tested microjet diameter ; a global increase of the SPL reduction with the mass flux ratio r_m, with a local maximum whose location varies from one curve to another. The comparison between the three diameter is delicate, because the best configuration in terms of SPL reduction depends on the value of r_m considered. Using the parameter r_m, the efficiency of the microjet diameter cannot be determined.

Figure 8(c) and 8(d) provide therefore the evolution of the SPL reduction with $r_m^\bullet$, based on a scaling of r_m to obtain the mass flux ratio equivalent to the $d = 1mm$ case, $r_m/d^2 \times 10^{-6}$. In other words, $r_m^\bullet$ is directly linked with the equivalent microjet velocity u_{eq}, knowing $r_m^\bullet = \pi/4 \times 10^{-6}\ u_{eq}/\Phi$, with the main jet volume flux Φ. We now observe a scaling of the local maxima for the three microjet diameters considered, obtained for $r_m^\bullet$ of about $2\ 10^{-4}$; that local maximum may then directly result from a microjet velocity effect. In particular, transition between subsonic and supersonic microjet flow in the microjet nozzle seems to appear for the range of $r_m^\bullet$ considered.

We also note the efficiency of the comparison between the microjet diameters in terms of SPL reduction with the representation implying $r_m^\bullet$. For a given value of $r_m^\bullet$, the noise reduction is an increasing function of the microjet diameter, for the range of diameters under the scope of this study. This tends to confirm the importance of the mass flux per microjet on the noise reduction.

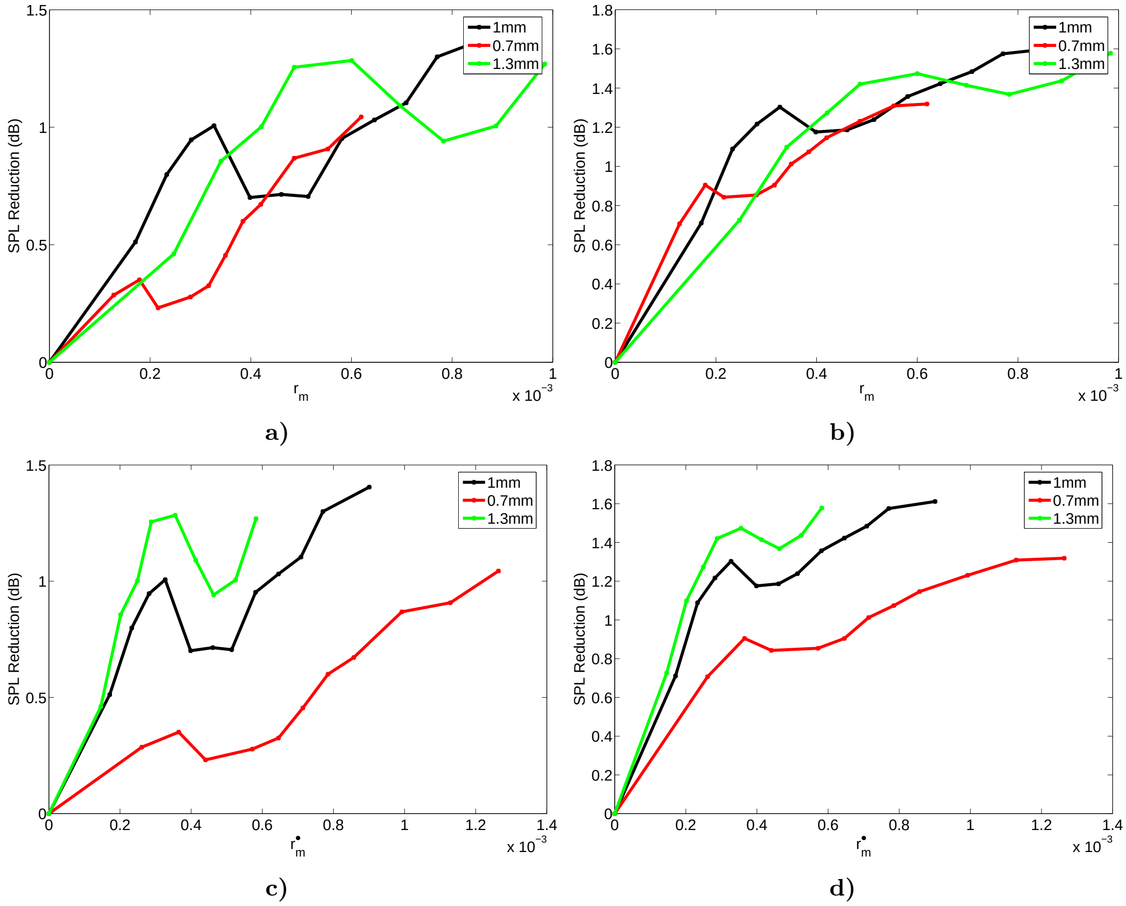

Fig. 8 Evolution of noise reduction for different microjet diameters : 0.7 mm, 1 mm, 1.3 mm with :
- mass flux ratio r_m ; (a) for $\theta = 30°$ and (b) for $\theta = 90°$.
- d=1mm-equivalent mass flux ratio $r_m^\bullet$ (*i.e.* $r_m/d^2 \times 10^{-6}$) ; (c) for $\theta = 30°$ and (d) for $\theta = 90°$.
Jet Mach number $M_j = 0.9$; Number of microjets : 18 ; Impacting angle : 45°.

Conclusions

The experimental investigation on jet noise reduction by use of impinging microjets was carried out in the supersonic anechoic facility of the Centre Acoustique, LMFA - École Centrale de Lyon and four parameters of the microinjection system were investigated. The study of the injected mass flux per microjet r_m - the only non-geometric parameter - reveals the existence of a local maximum in the Sound Pressure Level reduction, included in a global increase with r_m. Thanks to an adaptated scaling of the data, the different microjet diameters tested in these experiments indicates that this typical behaviour would be linked to flow transition from a subsonic microjet to a supersonic microjet, critical conditions being obtained at the microjet nozzle. A logical and complementary investigation will then characterize the microjet flow by means of shadowgraph techniques, to visualize the exhaust conditions of the microjet for a given mass flux.

The study of the microjets layout, for a given number of microjets and a given mass flux per microjet, indicates no measurable azimuthal directivity of SPL reduction at the angle $\theta = 30°$ and $\theta = 90°$. The examination of the associated spectra indicates that directivity effects exist and concerns frequency above 5 kHz, which are not decisive for SPL reduction. This illustrates a global effect of the microjets in the low frequency range and a local effect for higher frequencies.

The study of the number of blowing microjets also highlighted the dependency on the microjet mass flux of the configuration giving the maximum noise reduction. The maximum number of microjets do not imply a maximum SPL reduction, which imply that flow interaction between too close microjets may limit their efficiency. Flow measurements by means of stereoscopic Particule Image Velocimetry (2D-3C) will be realized to validate, in addition to previous measurements (Castelain *et al.*[6]), that conclusion of this acoustic study.

Références

[1]C.K.W. Tam. *Aeroacoustics of flight vehicles ; Volume 1 : Noise sources*, chapter Jet Noise Generated by Large-Scale Coherent Motion, pages 311–390. H.H.Hubbard, 1995.

[2]V.H. Arakeri and A. Krothapalli. On the use of microjets to suppress turbulence in a mach 0.9 axisymmetric jet. *J. Fluid.Mech.*, 490 :75–98, 2003.

[3]T. Castelain, M. Dietrich, J.C. Béra, and M. Sunyach. Contrôle par microjets d'une couche de mélange : exploitation de mesures PIV synchronisées. In *40ème colloque d'Aérodynamique appliquée, Toulouse, France*, mars 2005.

[4]T. Castelain, J.C. Béra, and M. Sunyach. Noise reduction of a Mach 0.7-0.9 jet by impinging microjets. *C.R.Mécanique*, 334 :98–104, 2006.

[5]E. Gutmark, W.B. Callender, R. Szasz, L. Fuchs, S. Martens Numerical study of fluidic injection for noise reduction In *9th CEAS-ASC Workshop, Stockholm*, November 2005.

[6]T. Castelain, J.C. Béra, and M. Sunyach. Noise reduction of a Mach 0.7-0.9 jet by impinging microjets. In *9th CEAS-ASC Workshop, Stockholm*, November 2005.